Prague, 16 April 2020

Dear Editor,

Thank you for the helpful and positive reviews of our submission Monitoring crustal CO2 flow: methods and their applications to the mofettes in West Bohemia to Solid Earth.

Below, and in the replies to the referees, we reply point-by-point to the reviewer's comments. And in the annotated manuscript below we show the tracked changes.
We addressed all the reviewer's suggestions and made few further cosmetic changes.

We hope the new revision will meet the requirements for accepting our paper for publication.

Best regards,
Tomas Fischer and coauthors

Anonymous Referee #1

Thank you for your helpful comments. We address all of them in our replies below and in most cases have modified the manuscript accordingly, which is in each case indicated in our reply.

Ad Specific comments

38: Fig. 1: The map: the marked distribution of granite is not complete. And it is a questionable presentation: what is important: relief or lithology- I suggest only one of them. The northern most mofettes in Fig. 1(latitude > 50.2)? They are really mofettes? Please check it.
Thank you for this comment, there was a mistake, and we have removed the two mofette symbols from the map.

56-62: at the end of these sentences, the authors should add here the sentences of the lines 73-81 for a better overview about the gas isotopic features.
Thank you for this suggestion, we moved the paragraphs accordingly, which also allowed to remove one sentence.

61: what is the meaning of "... high 3/4 He ratios..." ?
Now, after rearranging the paragraph, it gets clearer.

65: similar as above: What is high gas flow ? , see also line 73 and 75: unclear.
We have indicated the daily discharge of dozens of tons of gas

67: "the ascent of gas" – Numerous studies show that the earthquake swarms are related to the ascent of gas? This assumption has no evidences in my opinion or please, indicate the references.
Our formulation reads precisely "numerous studies of the local earthquake swarms show that they may be related to pressurized fluids in the crust and the ascent of gas". First, we mention fluids in general and only then gas. And we cite these studies in the next sentence. So, we decide to keep the sentence as it is.

73 “gases produced”, this terminus is may be correct but not usual for the characterization of natural degassing sites, see also line 108 & 405
Thank you, we changed to discharge (the first occurrence exists no more because the sentence was removed)

104: please add: (see Fig. 1)
OK, added.

110: what means “deep root” zone of mofettes? The origin of CO2 is known.
Yes, the gas is most probably of mantle origin. But here, we have in mind the mofettes, compared to diffuse degassing. In particular the fast coseismic reaction of the mofettes, which indicates that the CO2 origin is deeper than hypocenters, but nothing about the mantle origin.

201 “Within a few months” should be changed into “ Within a few days...” ?
No, the onset of increase started 4 days after the first event (mainshock) and continued for about three months, which underlines its significance.

294 & 295: This explanation is may be correct for mineral springs with a continuous gas/water discharge. However, mofettes can be considered as gas dominated migration path. It means that the CO2 will migrate as gas phase with over-pressure above the supercritical point. The water phase content will be of minor importance here. The groundwater horizons are the barriers and the beginning of the bubble creation which depends on the pressure ratios of gas and the water column if the maximal solubility in water is reached. This effect can be observed in submarine gas vents.
Thank you for this comment; we added a sentence “or in the presence of significant water discharge, such as in mineral springs.” to the end of the first paragraph of 2.4 to take this into account.

300: the driving force for gas flow is the hydraulic pressure gradient and the density contrast
Thank you for the comment; we had in mind “steady flow of the dissolved CO2” and have modified the text accordingly.

354: the section 2.6: the interpretation with the barometric efficiency is an interesting approach. Because of “the many unknowns in this regard”, a simplified way could be helpful in this context. What about this comparison: show an additional graph with the result of pressure head (in mbar) minus the atmospheric pressure (in mbar).
*The reviewer is right that such a plot might be illustrative. However, in Fig. 7a we show pressure_head minus 0.76*atmospheric_pressure, which is very similar and possibly better, we believe.*

387-391 these lines should be at the end of this section.
Thank you, we moved these lines accordingly.

427&428: The authors claim the increase of gas discharge as anomalous effect of different reasons except the anomalies as “probably merely accidental” at two sites (Soos and Bublák) during the summer 2016. These anomalies occurred a few weeks after the gas flow increase at Hartoušov due to the drilling process and the influence to the hydraulic regime. An assumption or specific interpretation should be added. Please think about the fluid interaction of the deeper horizons in the area (Cheb basin). For example, the gas eruption at the drill site H11 in the year 1957 induce an anomalous gas discharge and variations in the water levels in Františkovy Lázneˇ, about 2 km far. A reduced water table at the Hartoušov drill site could influence the hydraulic pressure regime in the nearby Cheb basin. This influence could trigger the ex-solution of CO2 of the water table with a temporal delay at other locations (mofettes), similar to the

atmospheric pressure effect.
The eruption in 1957 and drilling in 2016 were rather different in scale. In 1957 the eruption lasted for several days with water fountain of about 50 m height compared to very small and short gas leakages during the 2016 drilling.

464: Please take into account also that the strong drought period during the last summer reduces the level of the surrounding ground water table. This hydraulic pressure reduction induces an addition gas release as diffuse compo- nent and could reduce the total amount of gas discharge at the monitoring site.
We newly checked this influence by comparing the records of gas flow and water level in three sites: Hartousov mofette, Bublak and Soos.
In the Hartousov mofette similar decay of water level and gas flow rate is visible until about February 2018. The later anticorrelation is probably caused by malfunction of the level logger (temperature dependent).
Bublak and Soos show water level minima in summer 2018 and 2019, which partially correlate with the lowered gas flow in summer. However, no clear relation is found for 2017.
Because of unclear relation we do not show this graph in the paper. We added few sentences commenting on this possible influence to the Discussion.

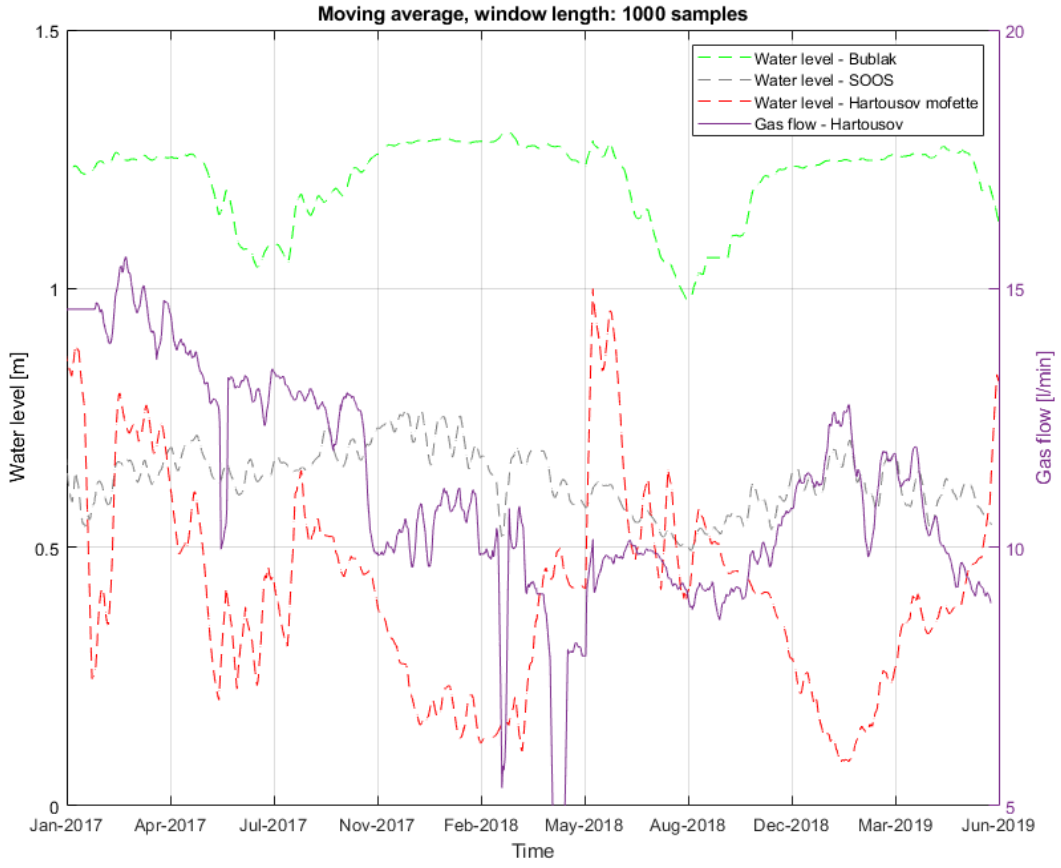

477: because of missing evidences of this process, please add "... indicates the possible presence of..."
We believe that the verb 'indicates' is a sufficient way to indicate that it is not fully proved (compared to verbs like proves, documents, etc...)

Ad Technical comments

CO2 – should be written with 2 subscript. The names of the ref- erences in the text should be outside the brackets, e.g. Fischer et al. (...), see line 68, 250, 259 a.s.o.
Thank you, corrected

439: considered as an 493 "discharges" is a better term here than "emanations"
Thank you, corrected

564 this reference is not mentioned in the text A few typesetting mistakes in the reference list
Thank you, corrected

The figure captions should be not in bold
Thank you for this comment, this occurred by mistake, now it has bee corrected.

Anonymous Referee #2

Thank you for your helpful comments. We address all of them in our replies below and in most cases have modified the manuscript accordingly, which is in each case indicated in our reply.

Ad Comments

…For example, a statement about the performance of resistivity measurements, which were also used to estimate the gas bubble fraction although in a different set-up, would be interesting…
We added few sentences to the end of Discussion commenting on the performance of the resistivity method.

P2 L50: Could you please specify which fault zone is meant here?
Thank you, this was not indicated. We clarify that this is related to the hypocenter trend.

Table 1. CarbonNet monitoring network: Hartoušov, the 105.8 m deep borehole is not mentioned in the description of the network in the main text (unless I missed it). Is the borehole used as the reference borehole for the integral method described in the following?
Thank you for this comment. No, this borehole is operated in a closed regime, so the integral method cannot be tested there. We added few sentences to clarify the origin of the borehole, in particular:
„In 2016, a 105.8 m deep borehole was drilled in the Hartoušov mofette with the aim of studying geo-bio interactions (Bussert et al., 2017). It showed a CO2 overpressure of 5 bars and was converted to a closed monitoring borehole with continuous measurements of downhole pressure and temperature and wellhead pressure. A broadband seismometer was installed in 70 m depth in the year 2019"

P6 L183: "ceiling of the aquifer" the term seems strange to me, I assume it means simply the top of the aquifer.
OK, we changed to top.

P9 LL 260 – 264: ".... that the gas bubbles have to appear at the penetrated section of the Hartoušov borehole. This allows us to determine the mean volumetric fraction of the bubbles using eq. (3) with h1(t) = hm(t) being the hydraulic head measured at the depth dm = 4m, and h2(t) = he(t) being the hydraulic head measured in any depth below the bubble entry depth, which we suppose to be at the upper part of the penetrated section at de = 20.5m (Fig.3)."
The statement is confusing to me. If the gas bubbles enter the borehole at the penetrated

section, how can the upper part of the penetrated section be below the bubble entry depth? Is the hydraulic head for he actually measured in the Hartoušov borehole or in the reference well mentioned before? I assume the latter is the case according to Figure 4. Could you please clarify the text here?
You were right that the formulation was confusing. Our understanding is that the bubbles enter the borehole at the upper edge of the perforation, which was not clear before. Now we slightly changed the wording by modifying –'in any depth below the entry point' to 'at the bubble entry depth (or anywhere below)'

P10 L 307: What is the observed mass flux at the teste site?
Based on the measurements of Nickschick et al. (2015) (2-100 tons/day over an area of 350 000 m²) the flow rate through the borehole section would be in the order of 1E-8 kg/s. We added this estimate to the text.

P 10: Section: Laboratory test of bubble fraction method: Could you please state clearly here which bubble fraction method was tested in the laboratory, the integral or the differential method? I assume the latter is the case.
You are right, we mention it now in the text.

P 11 LL 346 – 350 (Section: Laboratory test of bubble fraction method): I assume the statement, that the integral method performs better than the differential method, is purely based on the observed correlation of the field data and not supported by the laboratory tests.
Yes, the reviewer is right because the integral method could not have been tested in the laboratory.

Although, I agree with the statement it seems to be a bit out of context here.
Thank you for this comment. The section 2.5 in fact deals both with the laboratory tests and with the tests at Hartoušov. Accordingly, we renamed the section to 2.5 Tests of bubble fraction method

Furthermore, why is a different time window utilized for the differential method in Figure 5 and Figure 6?
In Fig. 5 the aim was to find the volumetric fraction values with highest possible range so that we can compare the results with laboratory results – that's why time windows from 2016 (differential method) and 2018/2019 (integral method) were chosen. In case of Fig. 6, where we compare only integral and differential method itself, our aim was to choose the same time interval for both methods. Unluckily, due to many technical issues, we were only able to choose the plotted time windows (Jun-Sep 2018 and Jan-Apr 2019), which are close to each other and have approximately the same length.

Maybe a separate section discussing the differences in more detail would be better here including the statement on P13 LL 432 – 436, which I assume refers back to Figure 6 and not Figure 5.
Thank you for this comment. In fact, the discussion of Figs. 5 and 6 was a bit mixed up. Now we corrected the figure number from 6 to 5 and added a sentence introducing Fig. 6.

P12 LL 385-386: This statement should be followed by paragraph P12 LL 392-399. The small rearrangement would make it easier for the reader to follow, that there is a large effect on the data due to barometric pressure variations and that these have to be corrected. Maybe that could also be explicitly mentioned, although it is implicitly clear.
We have rearranged it accordingly, also in agreement with the Rev#1 recommendation.

P8 L238 and 243: φ_0 should be capitalized
Thank you, we have corrected it

P10 LL 319-321: Figure 5 should be referenced here.
Thank you, we have added it

P11 L338: This should be Figure 5 and not Figure 6.
Thank you, we have corrected it

Monitoring crustal CO_2 flow: methods and their applications to the mofettes in West Bohemia

Tomáš Fischer, Josef Vlček, Martin Lanzendörfer
Charles University, Faculty of Science, Prague, Czechia

Abstract Monitoring of CO_2 degassing in seismoactive areas allows the study of correlations of gas release and seismic activity. Reliable continuous monitoring of the gas flow rate in rough field conditions requires robust methods capable of measuring gas flow at different types of gas outlets such as wet mofettes, mineral springs and boreholes. In this paper we focus on the methods and results of the long-term monitoring of CO_2 degassing in the West Bohemia/Vogtland region in Central Europe, which is typified by the occurrence of earthquake swarms and discharge of carbon dioxide of magmatic origin. Besides direct flow measurement using flowmeters, we introduce a novel indirect technique based on quantifying the gas bubble contents in a water column, which is capable of functioning in severe environmental conditions. The method calculates the mean bubble fraction in a water-gas mixture from the pressure difference along a fixed depth interval in a water column. Laboratory tests indicate the nonlinear dependence of the bubble fraction on the flow rate, which is confirmed by empirical models found in the chemical and nuclear engineering literature. Application of the method in a pilot borehole shows a high correlation between the bubble fraction and measured gas flow rate. This was specifically the case of two coseismic anomalies in 2008 and 2014, when the flow rate rose during a seismic swarm to a multitude of the pre-seismic level for several months and was followed by a long-term flow rate decline. However, three more seismic swarms occurring in the same fault zone were not associated with any significant CO_2 flow anomaly. We surmise that this could be related to the slightly farther distance of the hypocenters of these swarms than the two ones which caused the coseismic CO_2 flow rise. Further long-term CO_2-flow monitoring is required to verify the mutual influence of CO_2 degassing and seismic activity in the area.

Deleted: emanations

Formatted: Subscript

Formatted: Subscript

1. Introduction

Long-term monitoring of crustal fluids activity provides a unique opportunity to better understand the relationships among tectonic processes, seismic activity and migration of fluids in the Earth crust. Carbon-dioxide of deep origin represents a link between deep seated magmatic sources of CO_2, the fluid migration paths in the crust, which are controlled by the tectonic stress field, and the earth surface. The presented study is focused to monitoring of CO_2 degassing in the West Bohemia/Vogltand area, which is located in the western part of the Bohemian Massif (BM), the largest coherent surface exposure of basement rocks in central Europe. The western BM is hosting a junction of three tectonometamorphic units, Saxothuringian, Teplá-Barrandian and Moldanubian (Franke, 2000). It is intersected by two regional tectonic structures, the NE-SW trending Eger Rift (ER) and NNW-SSE trending Mariánské Lázně Fault (MLF) (Fig. 1).

The Tertiary ER is a 300 km long striking structure characterized by elevated heat flow and Cenozoic volcanism and its formation is thought to be related to Alpine collision (Ziegler, 1992). The Late-Variscan MLF was reactivated several times during the geological history up to Cenozoic when it participated in the formation of the Cheb Basin (CB). CB is typified by a blocky structural fabric due to a network of faults. Besides the NNW and NW morphologically expressed marginal faults also faults striking NE, E-W and N-S were identified within the basin (Špičáková et al., 2000; Bankwitz et al., 2003).

The present geodynamic activity is manifested by earthquake swarms, massive CO_2 degassing of mantle origin and Quaternary volcanism (Fischer et al., 2014). Seismic activity in the form of earthquake swarms is concentrated in the area of CB, in particular the Nový Kostel focal zone (Fig. 1), where more than 80% of seismic energy is released in frames of the whole seismogenic region. Here the hypocenters form a N-S trending, steeply dipping belt in the depth range from 6 to 10 km; however, no clear fault outcrop has been identified that would match the focal zone geometry. The prevailing focal mechanisms coincide very well with the orientation of the fault zone striking 169° derived from the hypocenter trend. Inversion of focal mechanisms for stress field yields maximum compression direction in the range N135–155°E, which coincides well with the average direction N144°E in Western Europe (Fischer et al., 2014). This direction is however parallel to the strike of the MLF, which indicates a passive role of the MLF in the present stress field (Vavryčuk, 2011).

The strongest earthquakes usually do not exceed M_L 4.5, as was the case of all the eight major instrumentally recorded swarms between 1985 and 2018.

The concentration of the geodynamic phenomena in this small region is not clearly understood. Some authors relate this seismic activity to intersecting crustal faults (e.g., Bankwitz et al., 2003) or to fluids of mantle origin (e.g., Bräuer et al., 2003; Babuška et al., 2016), which could originate from active magmatic underplating (Hrubcová et al., 2017). The degassing occurs in the form of CO_2-rich mineral waters and wet and dry mofettes in several degassing fields. Carbon dioxide is the carrier phase for mantle-derived minor components such as helium, the isotope ratios of which are the best tool to determine whether the fluids are of crustal or mantle-derived origin; high $^3He/^4He$ ratios indicate that ascending gases are of mantle origin (Bräuer *et al.*, 2003). The highest portions of mantle-derived helium (up to 6 R_a, where R_a corresponds to the $^3He/^4He$ ratio of the atmosphere) were found in the CB; the KV degassing center has the lowest $^3He/^4He$ ratios of 2.5 R_a. Lower He-isotope ratios (e.g. $^3He/^4He < 6Ra$) probably reflect the gas mixing

Deleted: of

Deleted: The gases produced in the West Bohemia/Vogtland mineral springs and mofettes show high $^3He/^4He$ ratios; these are significantly higher than the average continental crust, indicating their mantle-derived origin. Also, the $\delta^{13}C$ values in the CO_2-rich gas escapes indicate their origin in the upper mantle (Weinlich *et al.*, 1999; Bräuer *et al.*, 2003).

with crustal-derived He along fluid pathways (Bräuer *et al.*, 2008). Also, the $\delta^{13}C$ values in the CO_2-rich gas escapes indicate their origin in the upper mantle (Weinlich *et al.*, 1999; Bräuer *et al.*, 2003). CO_2 flow monitoring in West Bohemia has been conducted since the 1990s in a rather discontinuous way. The longest-running observation project is probably the monitoring of Radon activity in Bad Brambach (Heinicke and Koch, 2000; Koch et al., 2003), which has been conducted since 1989.

Gas flow is concentrated in three degassing centers: Cheb Basin, Mariánské Lázně, and Karlovy Vary (KV) (Weinlich *et al.*, 1999; Geissler *et al.*, 2005; Kämpf *et al.*, 2007). They are characterized by a high gas flow with daily discharge of dozens of tons of gas (Nickschick et al., 2015) with CO_2 concentrations of more than 99 vol. %. Cheb Basin also has the highest concentration of seismic activity, which makes it ideal for studying the relations between seismicity and gas flow. Interestingly, many studies of the local earthquake swarms show that they may be related to pressurized fluids in the crust and the ascent of gas. This has been pointed out by numerous researchers including Špičák and Horálek (2000), Hainzl and Fischer (2002), Fischer and Horálek (2005) and Hainzl et al. (2016), based on space-time analysis of the seismicity, Horálek et al. (2002), Vavryčuk (2002) and Vavryčuk and Hrubcová (2017), on the basis of moment tensor analysis, and Dahm and Fischer (2014), and Bachura and Fischer (2016), based on Vp/Vs analysis of the volume of hypocenters. The last two studies show that compressible fluids are required to explain the low velocity ratio observed in the course of seismic activity.

Another long-time monitoring was carried out as part of the "Research of CO_2 pressure field in the area of West Bohemian spas" project funded by the Ministry of the Environment of the Czech Republic from 1996 to 2005. Gas flow in open boreholes and gas pressure in closed boreholes was monitored at 11 gas escape sites in the Cheb Basin and near Mariánské Lázně (Škuthan et al., 2001, Hron et al., 2006). Monitoring of pressure in a closed well was preferred at many project sites since the functioning of mechanical flowmeters was unreliable due to condensation and freezing. A different type of CO_2 flow monitoring was carried out by Faber et al. (2009), who measured diffuse gas flow by determining CO_2 concentration in soil gas at two stations in the Nový Kostel fault zone. CO_2 flow monitoring was also conducted by Heinicke (personal communication) in the Bublák mofette from 2008 to 2014 by recording the acoustic noise of bubbles below the water table, a method which is similar to that used by Koch et al. (2003). No convincing observation of seismogenic CO_2 flow anomaly was, however, presented in the above-mentioned studies.

Mapping of CO_2 emanations was conducted in the area by Nickschick et al. (2015). They used an infrared gas analyzer and accumulation chambers to measure CO_2 flux and CO_2 soil concentration in the mofette field of Hartoušov and found that the diffuse gas flow in dry vents accounts for a high portion of the mofette field's total gas production.

The measurement of CO_2 flow presented in this paper began in 2009 in the Hartoušov mofette field with the use of a laboratory chamber flowmeter. Despite problems from the condensation of moisture and freezing temperatures, which resulted in time series gaps, we observed a massive post-seismic CO_2 flow increase shortly after the first M_L 3.5 mainshock of the 2014 seismic sequence. A comparison with the fault valve model showed a striking fit, which indicated that the earthquake fracture released gas accumulated in the reservoir beneath hypocenters (Fischer et al., 2017). This gave us a reason to extend the monitoring and test different, more durable, gas flow measurement methods.

In this paper, we introduce the principles for our approaches and give a basic comparison of them. We also present

Deleted: numerous

Deleted: The gases produced in the West Bohemia/Vogtland mineral springs and mofettes show high $^3He/^4He$ ratios; these are significantly higher than the average continental crust, indicating their mantle-derived origin. Also, the $\delta^{13}C$ values in the CO_2-rich gas escapes indicate their origin in the upper mantle (Weinlich *et al.*, 1999; Bräuer *et al.*, 2003). The highest portions of mantle-derived helium (up to 6 R_a, where R_a corresponds to the $^3He/^4He$ ratio of the atmosphere) were found in the CB; the KV degassing center has the lowest $^3He/^4He$ ratios of 2.5 R_a. Lower He-isotope ratios (e.g. $^3He/^4He < 6Ra$) probably reflect the gas mixing with crustal-derived He along fluid pathways (Bräuer *et al.*, 2008).

Deleted: CO_2 flow monitoring in West Bohemia has been conducted since the 1990s in a rather discontinuous way. The longest-running observation project is probably the monitoring of Radon activity in Bad Brambach (Heinicke and Koch, 2000; Koch et al., 2003), which has been conducted since 1989.

the data recorded from the Hartoušov, Bublák, Soos and Prameny stations (see Fig. 1) and evaluate their response to air pressure and temperature and their possible relation to seismicity.

2. Data and methods

Two types of CO_2 degassing are observed in West Bohemia/Vogtland: (i) diffuse gas flow in soil and (ii) massive gas discharge in mofettes and mineral springs. While gas diffusion in soil is influenced by soil moisture and other local conditions, among other factors, gas flow in massive sources is independent of environmental conditions and should reflect the influence of the gas source at in the depth. The deep roots of CO_2 mofettes were also documented by a massive increase in CO_2 flow in the Hartoušov mofette that began about four days after the start of seismic activity in 2008 and 2014 (Fischer et al., 2017). This points to the relatively fast speed of gas migration in the upper crust and qualifies mofettes as favorable places to monitor the amount of leaking gas. Since 2015, the current monitoring at Hartoušov has been extended to other places in order to provide robust measurements capable of recording possible future gas anomalies at multiple sites. Because the conditions differed among the monitored sites, different measurement methods were designed. In this study, we distinguish between *direct* and *indirect* gas flow measurement methods (Camarda et al. 2006). The direct methods directly record the volume of gas per minute and require that gas flow be captured by a funnel or borehole. The indirect methods either involve deriving gas flow from the bubble fraction in water (pressure probes are placed beneath the water table), or rely on measuring gas overpressure in a closed borehole or, finally, they calculate CO_2 flux from the concentration of gradients in the soil (Baubron et al., 1990). The dynamic concentration method is based on measuring the CO_2 content in a mixture of soil gas and air obtained by a special probe placed vertically in the soil. The dynamic concentration is proportional to the soil CO_2 flux according to an empirical relationship, which depends on soil permeability (Gurrieri and Valenza, 1988).

Figure 1 .

2.1 Monitoring network

Five gas escape sites were monitored in the period described: *Hartoušov, Bublák, Soos, Dolní Částkov* and *Prameny* (see the map in Fig. 1 and photos in Fig. 2). While the first three are located in mofette fields, the remaining are boreholes which tap mineral spring sources.

The pilot site of *Hartoušov* is located in a wooden hut above a 28.2 m deep F1 borehole, which taps a CO_2 saturated, pressurized aquifer. The plastic borehole casing, with an inner diameter of 115 mm, is perforated in the depth range of 20-28 m. Water level measurements date back to 2007, and gas flow has been measured here using a drum chamber gas flowmeter since 2009. The sensitivity of this type of instrument to environmental conditions (freezing or evaporation of the working liquid) caused gaps in the recorded time series. Since 2013, there have only been brief gaps thanks to the use of a different type of working liquid, improvements in the condenser separation and thermal insulation. This direct field gas flow measurement is used as a reference for testing different flow measurement devices prior to their installation at other sites. Additional permanent measurements include water pressure in several depth

Deleted: production

Formatted: Subscript

levels, water temperature and air temperature and pressure. In 2016, a 108.5 m deep borehole F2 was drilled in the Hartoušov mofette with the aim of studying geo-bio interactions (Bussert et al., 2017). It showed a CO_2 overpressure of 5 bars and was converted to a closed monitoring borehole with continuous measurements of downhole pressure and temperature and wellhead pressure. A broadband seismometer was installed in 70 m depth in the year 2019.

The *Bublák* station has been located in a natural mofette in a swamp since 2015. To avoid interfering with natural conditions at this site, the equipment is buried underground, which does not allow for direct gas flow measurement. Instead, the differential water level is measured and used as a proxy for the volumetric fraction of free gas in water, see section 2.3. Because of the rising bubbles, the water does not freeze in winter, making this measurement quite stable. The *Soos* station has been located in a natural mofette field since 2015, and the gas from a single mofette is captured by a funnel allowing for direct gas flow measurement. The small size of the metal box shelter and the need to use battery power, however, do not make it possible to prevent the freezing of the system in winter. The water level and temperature in the mofette and the volumetric fraction of free gas are measured here using an electric resistivity probe. In *Dolní Částkov*, the gas escapes both through a shallow borehole and the surrounding soil, which makes the flow measurements rather unstable. The *Prameny* station is located on top of a 100 m deep closed borehole (HJ-3A, drilled 1994) with degassing mineral water. Conditions at this site allow only for the measurement of the water level, temperature and wellhead gas pressure, which have been available since 2009.

Figure 2 .

Table 1. CarbonNet monitoring network.

Station name and code	Environment	Methods
Bublák *BUB*	*Natural mofette*	*Water temperature, two pressure heads (sensor depths 0.7 and 1.4 m)*
Hartoušov *HAR*	*30m deep open borehole VP8303 (F1)*	*Air temperature, barometric pressure, three pressure heads (sensor depths 4.45, 5.45 and 27.2 m), water temperature, gas flow rate, differential pressure in the well*
	108.5m deep closed borehole HJB-1 (F2)	*Pressure head (sensor depth 92m), water temperature, absolute wellhead pressure, seismometer*

Deleted: 5.

Prameny *PRA*	*100m deep open borehole* *HJ-3A*	*Pressure head (sensor depth 4.5 m), water temperature, absolute wellhead pressure*
Soos *SOO*	*Natural mofette*	*Pressure head (sensor depth 1.5 m), water temperature, water resistivity*
Dolní Částkov *DCA*	*10 m deep open borehole*	*Gas flow rate*

2.2 Direct CO_2 flow measurement methods

Long-term gas flow monitoring in the field must meet various requirements. It should provide sufficiently accurate data of gas flow, which may contain dirt particles and moisture in changing field conditions of temperature, humidity and air pressure. The presence of carbon dioxide further creates a highly corrosive environment, which the sensors should withstand. Commercial flowmeters are usually not designed to meet these demands. We have tested (at SOOS and Dolní Částkov stations) the *MEMS* (Micro-Electro-Mechanical Systems) *flowmeter*, which is based on heat convection in moving gas. It works on the principle of a wheatstone bridge, where changes in the resistivity of the resistor are measured according to the temperature changes caused by the flow of gas through a heater placed in the middle of the sensor (Dmytriw et al., 2007). These low-cost sensors, however, failed in our tests. None of the MEMS flowmeters tested measured for longer than 4 months, despite the installation of filters to capture solid particles and moisture from the gas before entering the sensor. A popular way of measuring gas flow is the *Venturi type flowmeter,* which works by measuring the drop-in pressure at a constriction in a tube. Our tests of similar devices failed due to temperature drifts of the sensor and electronics, which were of the same order as the CO_2 flow variations. Direct flow measurement methods also include the *acoustic method* based on the Doppler effect, which is commonly used for water flow measurement. This, however, does not appear to be suitable for gas, which contains fewer particles acting as diffractors than liquid.

The standard *flowmeters with rotating mechanical parts* driven directly by the gas flow were also found not suitable due to the corrosive CO_2 environment. Better performance was achieved with a *drum-type chamber flowmeter*, which contains a revolving measuring drum within a packing liquid (we use low-viscosity oil). The measuring drum compulsorily measures volume by periodically filling and emptying four rigid measuring chambers. This *chamber laboratory instrument* was found suitable for field measurement, where sufficient space and non-freezing temperatures can be guaranteed. It has been used as the primary flowmeter at the Hartoušov F1 borehole.

Deleted: station

2.3 Indirect CO_2 flow measurement methods

Gas pressure in a closed borehole

In a closed borehole tapping a gas-saturated aquifer an overpressure builds up whose magnitude has been speculated to reflect the amount of gas entering the aquifer from below (e.g. Hron and Škuthan, 2006). However, a profound discussion of how exactly the deep CO_2 leakage affects the measured overpressure is still absent, to the best of our knowledge. Considering a CO_2 flux $q = q_1 + q_2$ summing the flux through the top of the aquifer in the vicinity of the borehole, q_1 and the possible gas leakage through the borehole, q_2, and assuming simply that the borehole overpressure p is proportional to the both, then p follows the equation

$$p = \frac{q}{K_1 + K_2},$$

where K_1 and K_2 are the permeability factors related to the ceiling of the aquifer and to the borehole sealing, respectively. Hence the measured overpressure is proportional to the gas flux controlled by deep processes, but also influenced by the permeability of the superficial layer as well as by any possible leaks through the wellhead. In particular, any variation in sealing layer properties, caused e.g. by the actual weather conditions, is then directly projected onto the pressure measured.

Accordingly, in spite of the easy implementation of the pressure measurements in a closed borehole, we used this method only at the *Prameny* site, where technical and logistic conditions did not allow the installation and maintenance of a flow measurement. Excessive influence of K_1 on the measured pressure can be suppressed by introducing a controlled leakage in the wellhead, which ensures that K_2 is not small in comparison to K_1 as has been implemented at *Prameny* station.

Bubble fraction in water

We have used the bubble fraction monitoring method since observing a striking coincidence between the gas flow rate and groundwater level (see later in this paragraph) increase in the Hartoušov F1 borehole during the 2014 seismic sequence (Fischer et al., 2017). Within a few months after the beginning of the sequence, the gas flow rate in the borehole increased fivefold and the measured water level by more than 1 m. Since then, both quantities have indicated an overall gradual decrease back to their original levels.

Instead of the notion of groundwater level, adopted in Fischer et al. (2017) and other works, we stick to the more strictly defined terms *pressure head* and *hydraulic head* in the present paper, which is due a few explanatory comments. Within a steady water column resting in a borehole (or a narrow mofette), the hydraulic head (defined as the sum of the pressure head and elevation) is independent of the elevation and is referred to as the groundwater level, as it coincides with the elevation of the free water surface observed in the borehole. This is why the exact elevation of the actual placement of the pressure probes in the borehole is usually disregarded, and the term groundwater level is used somewhat loosely without risk of any confusion. In the case of a continuous bubbly flow through the borehole, however, hydraulic head is not a depth-independent quantity, but rather inevitably increases with elevation. An intuitive explanation is that the mean density of the water - gas bubbles mixture is markedly lower than that of water

Formatted: Subscript

Formatted: Subscript

Deleted: ceiling

Deleted: (

Deleted: ,

(this is, however, merely an approximation, see also section 2.5). Following this simple concept, the density of the mixture would be (disregarding the density of the gas CO_2 as negligible)

$$\varrho(z) = (1 - \phi(z))\varrho_w, \tag{1}$$

where $\phi(z)$denotes the volumetric fraction of bubbles in the water column profile at elevation z, and ρ_w stands for the mass density of the water in the well (say, clear water at a given constant temperature). Denoting by $\psi(z)$ the pressure head, related to the actual pressure $p(z)$ through $p(z) = \rho_w g\psi(z) + b$ with g being the gravitational acceleration and b the barometric pressure (Fig. 3a), and denoting by $h(z) = \psi(z) + z$ the hydraulic head, we assert that the difference in the measured pressures, pressure head and hydraulic head equals

$$\begin{aligned} p(z_1) - p(z_2) = p_1 - p_2 &= \int_{z_1}^{z_2} \rho(z)\, g\, dz \\ \Rightarrow\ \psi_1 - \psi_2 &= \textstyle\int_{z_1}^{z_2} \big(1 - \phi(z)\big)\, dz \\ \Rightarrow\ h_2 - h_1 &= \textstyle\int_{z_1}^{z_2} \phi(z)\ dz\,, \end{aligned} \tag{2}$$

i.e. the hydraulic head *h(z)* measured in the borehole increases with elevation by a factor equal to the volumetric fraction of the bubbles in the borehole profile. Here, for the sake of brevity, we abstract from the time dependence of all quantities.

Figure 3

The mean bubble fraction within the measured section of the water column can thus be defined as

$$\phi_{12} = \tfrac{h_2 - h_1}{z_2 - z_1} = 1 - \tfrac{\psi_1 - \psi_2}{z_2 - z_1} \tag{3}$$

As the ascending gas bubbles expand due to the decreasing pressure, both the volumetric flux of the gas and the bubble fraction $\boldsymbol{\phi}$(z) increase correspondingly with elevation. In order to obtain a quantity independent of the depths of the pressure probes, a further correction needs to be applied. A reasonable approximation can be obtained based on the following simplification. We assume that the gas expands isothermally, so that its volumetric flux is inversely proportional to pressure, and that the bubble fraction is approximately proportional to the volumetric flux, so that we can write

$$\phi(z) = \phi_0 \frac{p_0}{p(z)}$$

where Φ_0 represents the bubble fraction at the reference pressure p_0 (which we later set as 100 kPa). Further, approximating the pressure profile between the two pressure probes by a linear function

$$p(z) = p_1 + \frac{z - z_1}{z_2 - z_1}(p_2 - p_1)$$

we obtain (by substituting $\phi(z)$ to (2) and integrating) the formula for Φ_0, let us call this the projected bubble fraction,

$$\phi_0 = \underline{\phi_{12}} \tfrac{p_2 - p_1}{p_0 ln\,(\frac{p_2}{p_1})} \tag{4}$$

One should note that the quantity obtained here is subject to some uncertainty due to a number of simplifications, and that it only gives the approximated volumetric fraction and not the gas flow rate itself (see section 2.5).

In the Hartoušov F1 borehole, the pressure head had been measured until September 2018 by one pressure gauge in the depth of 8 meters, well above the bubble entry point. In Fischer et al. (2017), the corresponding hydraulic head was referred to as the groundwater level. As proposed in the paper, we split its time variation into two parts: the variation (a) of the hydraulic head $h_e(t)$ at the bottom of the bubble flow column and (b) of its increase through the column due to the gas bubbles. The optimal solution to obtain data for (a), which was implemented in Hartoušov F1 in late 2018, is to measure the pressure head in a depth beneath the bubble entry point directly by a dedicated pressure probe (Fig 3b). While direct measurement was unavailable, it was supposed that (a) is given only by the surrounding hydrogeologic situation and is unaffected by the gas flow. A single measurement of the pressure at the bubble occurrence depth by Fischer et al. (2017), corrected by a continuous pressure head record from a nearby observation well in Hrzín 8 km apart, which is not affected by the CO_2 gas flow, was used as $h_e(t)$. Note that $h_e(t)$ also describes the hydraulic head in any depth beneath the occurrence of bubbles. While Fischer et al. (2017) considered the possibility that the gas exsolution depth varies with time, we argue here (see section 2.4) that the gas bubbles have to appear at the penetrated section of the Hartoušov F1 borehole. This allows us to determine the mean volumetric fraction of the bubbles using eq. (3) with $h_1(t) = h_m(t)$ being the hydraulic head measured at the depth d_m = 4 m, and $h_2(t) = h_e(t)$ being the hydraulic head measured at the bubble entry depth (or anywhere below), which we suppose to be at the upper part of the penetrated section at d_e = 20.5 m (Fig.3).

In Fig. 4 the record of $h_e(t)$ and $h_m(t)$ and the resulting projected bubble fraction $\phi_0(t)$ defined by eq. (4) is shown for the whole period studied in Fischer et al. (2017). We refer to this method as the *integral method.*

Figure 4

The method presented above is applicable only in boreholes and narrow tube-like mofettes. The borehole should tap the underground water, and there should exist a continuous column of gas bubble flow from certain depth to surface. Also, independent measurement of the hydraulic head in the aquifer/reservoir beneath the bubble flow column should be possible, either in the same well or, at least, in a nearby well free of gas flow. These conditions are not fulfilled in natural mofettes, which are usually only less than 2 m deep and communicate with the surface water significantly. In such cases, the difference of pressure heads along a fixed depth interval *within* the bubble flow column can be measured and used to define the mean bubble fraction $\underline{\phi_{12}}(t)$ and the projected bubble fraction $\phi_0(t)$.

This *differential method* has been tested in the Hartoušov F1 well and Bublák mofette stations since 2015 using two analog water-level sensors attached at a 1-meter distance on a metal rod. The obvious disadvantage is that both measurements (instead of just one) are subject to fluctuation due to the bubbly flow, and that the noise in the resulting bubble fraction data is inversely proportional to the distance between the probes. To suppress the noise, an RC circuit with a 100 s time constant is applied.

An alternative way of determining the bubble fraction is based on the electric resistivity measurement of the water-bubble mixture. Unlike the pressure difference method, this method does not need to be focused on the vertical chain

Deleted: (
Deleted: ,
Deleted: (
Deleted: ,
Deleted: (
Deleted: ,
Deleted: in any depth below the bubble entry depth

of bubbles, but it can assess the fraction of bubbles in a 3D volume defined by the geometry of electrodes. For this purpose, two water resistivities are measured by a special probe in the mofette: the reference resistivity of the water free of bubbles R_R and the resistivity of the water-bubble mixture R_M. The bubble fraction is then derived as

$$\phi(t) = 1 - c\,\frac{R_R(t)}{R_M(t)}$$

where c is the geometric calibration constant. This type of measurement has been tested in the Soos mofette since 2015.

2.4 Depth of gas bubbles appearance

It is possible to speculate that the exsolution of the gas bubbles from the water with dissolved CO_2 takes place at a certain depth in the borehole, while below that depth the pressure is sufficient to contain the CO_2 in the dissolved phase. In this view, the exsolution depth d_e could vary in time, as considered by Fischer et al. (2017), following variations of $h_e(t)$ and of the CO_2 supply from the reservoir. Let us note, however, that such a scenario is only possible for gas fluxes much lower than those observed in the Hartoušov F1 borehole.

Assuming a steady flow of the dissolved CO_2 up through a borehole section with no penetration below d_e, two transport mechanisms can be considered, convection or molecular diffusion. As for convection, no driving force to induce a flow in a water column in a borehole, in particular no significant temperature variations, has been observed in the Hartoušov F1 borehole. The mass flux due to molecular diffusion, on the other hand, can be estimated as follows, and it appears to be very limited. Assuming that the concentration of the dissolved CO_2 in the resting water column increases with increasing depth as much as allowed by the increasing hydrostatic pressure (with the Henry's law constant being of the order of 10^{-5} kg m^{-3} Pa^{-1}, see Sander, 2015), then the corresponding diffusive flow rate (with the diffusivity being of the order of 10^{-9}m^{2}s^{-1}) through the borehole of the given cross-section area (say, 10^{-2} m^2) would be no more than of the order 10^{-12} kg s^{-1}. This is by four orders smaller than the mass flow rate through the borehole section of 1.6 10^{-8} kg s^{-1} estimated on the base of CO_2 flow measurements of Nickschick et al. (2015) who reports the daily flow rate of 50 tons for an area of 350 000 m^2. We thus infer that the gas bubbles enter the Hartoušov F1 borehole in its penetrated section, as we assumed in the previous section or in the presence of significant water discharge, such as in mineral springs..

2.5 Tests of bubble fraction method

The methodology for indirect gas flow measurement using pressure difference (the differential method) was first tested in the laboratory. The experimental setup consisted of an air pump connected with a valve for controlling the air flow, which was led to the bottom of a plastic tube with an inner diameter of 10.5 cm and a height of 2.5 m simulating the borehole. Two water pressure probes were installed at a fixed distance of 0.5 m on a vertical rod inside the tube and all the air from this tube was led to the chamber gas flowmeter. The air inflow was increased stepwise, and at each level the data were recorded for a period of 15 min using a 1Hz sampling rate. The gas flow ranged from 0 to 30

Deleted: gas

Deleted: flux

Deleted: Laboratory

Deleted: t

L/min, which corresponds to the volumetric flux ranging from 0 to 0.06 m/s. The observed mean bubble fraction appears to increase nonlinearly with the gas flow (Fig. 5). Note that the modification using (Eq. 4) is insignificant here, due to the fact that both pressure probes are at a depth of less than 1 m. The bubble fraction values are more scattered than the gas flow rate measured by the flowmeter. The resulting noise was partially suppressed by low pass filtering of the pressure data using an RC circuit with a time constant of 30 s and additionally by 1 min data sampling to smooth the water level values.

It is worth noting that the dynamics of bubbly flow in a borehole is quite a complex issue, which however appears to have been studied rather intensively in the chemical and nuclear engineering literature (see, e.g., Ghiaasiaan, 2008; Montoya et al., 2016). The simple considerations introduced in the previous text (Eq. 3 and 4) correspond to the drift-flux model for a vertical borehole, provided that the water flux through the borehole is negligible. In particular, any momentum exchange with the walls is ignored. While this approach is well justified for the bubbly flow regime observed with small gas fluxes, with increasing volumetric gas one observes different flow regimes of greater complexity, such as the slug flow and churn flow. As the bubbles ascend, they increase in volume, join each other merrily or even sadly split apart, their brief life being eventually cut short by obstacles such as the pressure probes dangling in the well; these are however out of the scope of this paper. Even in the bubbly flow regime, the relation between the bubble fraction ϕ and the volumetric flux of the gas bubbles u [m/s] has been described, e.g., by the following well established empirical relation (Zuber and Findlay, 1965).

$$\phi = \frac{u}{C_0 u + V_{gj}} \quad (5)$$

where $C_0 = 1.13$ and, assuming that the density of the gas is negligible when compared to that of water,

$$V_{gj} = 1.41 \left(\frac{\sigma g}{\rho_w}\right)^{1/4}$$

The curve in Fig. 5 is obtained by taking the surface tension for water and air at the laboratory temperature as $\sigma = 0.07$ N/m. It appears that the mean bubble fractions derived from our pressure probe data overestimate the void fractions given by the Zuber-Findlay model, in particular for low flow rates.

For comparison, we also show in Fig. 5 the projected bubble fraction data ϕ_0 plotted against the corresponding gas flow rates measured on the Hartoušov F1 borehole. The comparison to the laboratory data and to the Zuber-Findlay model reveals a discrepancy that indicates some need for further analysis, which is beyond the scope of the present study. Let us briefly note that the difference cannot be explained by the mere parametric differences from the laboratory setting such as the temperature, gas and water composition.

In Fig. 6 we compare the bubble fractions obtained on the Hartoušov F1 borehole using integral and differential methods. While it appears that the projected bubble fraction data from the Hartoušov F1 site cannot be directly inverted to obtain a reasonable gas flow rate estimate, it is important that they provide a fair correlation (see also Fischer et al. 2017 and Fig. 4 in their paper) and can thus provide a valuable gas flow rate proxy. As expected, the integral method data seems to perform better than the differential data (see Section 2.3). Note particularly the high noise of the latter and its lower correlation to the gas flow rate measurement (Fig. 6). Accordingly, using the pressure sensors at a larger distance, and, if possible, placing one of them below the bubble entry depth, seem preferable for indirect gas flow measurement.

Deleted: S.M.,
Deleted: , G.
Deleted: ,
Deleted: e
Deleted: e
Deleted: append to
Deleted: 6
Deleted: in
Deleted: site
Deleted: e
Deleted: append to
Deleted: less recent

Figure 5

Figure 6

2.6 Environmental effects

The measurements of CO_2 flow, CO_2 pressure and pressure head are influenced by environmental effects – mainly variations of temperature (diurnal, seasonal), changes of barometric pressure and tidal effects. Temperature and barometric changes are the most significant, since their influence can be local and can vary even among the stations of the network. Barometric and tidal loading of aquifers has been studied in detail (e.g. Jacob, 1939; Rojstaczer and Riley, 1990; Roeloffs, 1996). Here, we address the basic principles that are relevant to the pressure and production of the upstreaming gas. Both the confined and unconfined response of pressure head are characterized by the barometric efficiency E_B, which expresses the ratio of the change of the hydraulic head Δh caused by the barometric pressure change Δb

$$E_B = \rho_W \, g \frac{\Delta h}{\Delta b} \tag{6}$$

The net response is always a decrease in the hydraulic head with an increase in barometric pressure. The barometric pressure variations act directly on the open water level in the well and also on the formation composed of the mineral matrix and pore space filled by the water. As a result, the direct effect on the water level in the borehole is partially suppressed by the fraction of the external load borne by the formation water. Hence, the barometric efficiency can also be written as

$$E_B = \frac{\theta\beta}{\theta\beta+\alpha} \tag{7}$$

where α and β is the compressibility of the rock matrix and water, respectively, and θ represents porosity within the aquifer. Thus, barometric efficiency can be described as the fraction of specific storage derived from the compressibility of water or, equally, as the fraction of external load change borne by the formation either as compaction or expansion. Accounting for the range of fractured rock compressibilities, E_B of confined aquifers usually ranges between 0.2 and 0.7 (Todd, 1980) and may reach 1.0 for granite with a very low compressibility of the rock matrix (Roeloffs, 1996; Acworth and Brain, 2008). Note, however, that large values of E_B may as well correspond to large values of β; this fact is not addressed in the literature for the simple reason that it is usually the rock that varies from site to site and not the water. In this concern, the possible effect of the presence of the compressible CO_2 bubbles within the aquifer surrounding the borehole on the barometric efficiency is a question that has not been addressed in the literature, to the best of our knowledge.

Similarly, the barometric effect to the CO_2 discharge from an aquifer through an open well has not been studied either. One can expect that an increase in the pore pressure due to an increase in the barometric pressure allows for larger amounts of CO_2 to be dissolved in water, which in turn decreases the volume of CO_2 leaking into the well. Similarly, a decrease in barometric pressure may induce increased degassing. Note that there exist many unknowns in this regard, such as the flow paths of the gas ascending through the aquifer, the amount of the mobile and immobile gas bubbles in the porous space, etc. In the Hartoušov F1 borehole, a strong anticorrelation between the gas flow rate and the barometric pressure has been observed.

We correct the measured quantity f (pressure head or gas flow) for demeaned barometric pressure variations b using the equation $f_c = f - E_B (b - <b>)$. Barometric efficiency E_B is determined with the target of minimum cross correlation of f and f_c. To account for the possible time variation of E_B a sliding window of one day is used; see Fig. 7a for original and corrected records of pressure head and gas flow in Hartoušov F1. Fig. 7b shows the cross-correlation functions between barometric pressure and original and corrected records. The success of barometric correction is indicated both by removing the anti-correlation with air pressure and by minimizing short period variations in the corrected records. The mean barometric efficiency was 0.76 for the pressure head and 0.46 L/min/kPa for the gas flow.

Figure 7

Other external effects like diurnal temperature variations and Earth tides were found much weaker than the influence of barometric pressure. The volumetric fraction of bubbles is not affected by air temperature, since the sensors are placed in groundwater with an almost constant temperature. In addition, the periods of diurnal temperature variations and significant Earth tide components are significantly shorter than the expected durations of anomalies of deep-generated gas flow. Accordingly, we do not apply corrections for temperature variations and Earth tides.

Deleted: Other external effects like diurnal temperature variations and Earth tides were found much weaker than the influence of barometric pressure. The volumetric fraction of bubbles is not affected by air temperature, since the sensors are placed in groundwater with an almost constant temperature. In addition, the periods of diurnal temperature variations and significant Earth tide components are significantly shorter than the expected durations of anomalies of deep-generated gas flow. Accordingly, we do not apply corrections for temperature variations and Earth tides.

Deleted: ¶ ... [1]

3. Results of CO_2 flow monitoring in West Bohemia

The time series of gas production at all monitored stations, along with seismicity plot, are shown in Fig. 8. The record at Hartoušov F1 for the period from late 2007 to 2019 shows a long-term decrease interrupted by several abrupt massive increases in gas discharge. The maximum flow, reaching 50 L/min, followed the 2014 seismic sequence in late summer/autumn 2014; the minimum values, below 10 L/min, were observed prior to the 2014 seismic sequence and at the present time. The fast coseismic increase and long-term postseismic decrease are visible both in the gas flow and *integral bubble fraction* data determined using eq. (3) and (4) and are consistent with Sibson's fault valve model (Fischer et al., 2017). Note particularly the abrupt rise in gas flow and CO_2 bubble fraction during the M_L 4.4 seismic sequence of May – August 2014 and in bubble fraction during the October 2008 M_L 3.8 swarm. Next to these striking coincidences of seismic activity and CO_2 release we also find cases of strong seismic activity, which was not accompanied by a significant gas flow anomaly (see the M_L 3.4 swarm of 2011 and the most recent M_L 3.8 swarm of 2018). On the other hand, the CO_2 flow record shows a few positive pulses which are not related to significant seismic activity (Fig. 8b). The most striking one is the gas production increase in the period from the beginning of May till the end of July 2016, which is visible both in the gas flow and bubble fraction records. This is, however, undoubtedly of anthropogenic origin caused by drilling of the nearby 108.5 m deep F2 borehole at a distance of 40 m from the monitored F1 borehole, which drilling started on March 30 (Bussert et al., 2017). The drilling reached the top of a CO_2 pressured horizon at a depth of 80 m on April 21 and created a shortcut to the shallower aquifer, which was tapped by the monitored borehole. The three-month long gas increase thus represents a delayed response to a nearby drill. Another, less pronounced, positive pulse in the period from mid-September to late November 2016 is of unknown origin. A number of negative pulses and oscillations are found on the bubble fraction record alone, which lower the

Deleted: production

Deleted: HJB-1

Deleted: VP 8303

Deleted: ceiling

correspondence between the gas flow rate and the bubble fraction data and indicate a more complex relation between gas flow in a borehole and volume fraction of ascending bubbles, as already noted in section 2.5.

The records of gas *differential bubble fraction* data in Bublák and *resistivity-based bubble fraction* in Soos indicate in the monitored period since autumn 2015 a steady gas release with only a few bumps, which are most probably of local origin and related to the shallow character of the mofettes. Gas at these sites passes through approximately cylindrical vents of ~0.5 m diameter and ~1 m depth filled by surface water. The similarity of bubble fraction increase at Soos and gas flow increase at Hartoušov F1 in summer 2016 is most probably merely accidental, considering the anthropogenic origin of the rise at Hartoušov and the large mutual distance of about 5 km of these sites.

As mentioned in section 2.3, the integral method of bubble fraction measurement provides better results than the differential method. The latter suffers particularly from high noise caused by the placement of both pressure probes in a water column with flowing bubbles as shown in Fig. 6. One can also notice a better correlation of the integral method compared to the differential one. Unfortunately, due to technical problems, we were not able to perform this comparison for the same time window – so time windows of the same length (3 months) free of any technical issues were selected.

Deleted: 5

4. Discussion

The *barometric efficiency* E_B of the groundwater pressure head of 0.76, which we obtained, is relatively high. The high values of E_B are generally considered an indication of the small compressibility of the rock matrix that is typical for unweathered granite (Acworth and Brain, 2008). The target aquifer is formed by sedimentary formations of the Cheb Basin composed of sandstones and conglomerates with varying clay contents underlain by mica-schist basement (Bussert et al., 2017). The compressibility of these types of rocks is, however, 3 to 6 times greater than of granite (their bulk moduli range from 10 to 20 GPa compared to 50 GPa for granite). Using Eq. (4), porosity 30% and bulk moduli ratio of matrix and pore fluid equal to 5, one gets $E_B = 0.5$. The level $E_B = 0.76$ is reached for bulk moduli ratio of 15. Assuming the bulk modulus of aquifer rocks about 10 GPa, one obtains a bulk modulus of the fluid of only about 0.7 GPa, which corresponds to three times larger compressibility than for water. This could be explained by the presence of carbon dioxide in the groundwaters in gaseous phase and is worth further research.

The gas flow trend in Hartoušov after the 2014 seismic sequence shows signatures similar to those in the period before 2014, which followed the 2008 swarm. A similar, long-term overall decrease is followed by steady state behavior with an almost constant flow rate of about 10 L/min. In terms of the Sibson's fault valve model, this corresponds to the self-sealing phase of the fault due to mineral precipitation (Sibson, 1992) when pressure builds up and in combined action with tectonic loading results in increasing instability of the fault. This inevitably leads to later recurrence of fault failure in the form of seismic activity and regeneration of fault permeability. As indicated above, the coincidence of a massive rise in CO_2 flow and seismic activity has not been observed since the 2014 seismic sequence. Indeed, none of the earthquake swarms since 2014 have been accompanied by a distinct CO_2 degassing anomaly (Fig 8b). All in all, in the whole period of CO_2 flow monitoring in Hartoušov since 2007, five earthquake swarms with magnitude M_L larger than 3.0 occurred (2008, 2011, 2014, 2017, 2018) and only two of them (2008 and 2014) were accompanied

by a strong and long-lasting coseismic increase in CO_2 degassing. This is not surprising in general, because the fault valve mechanism might act only under certain circumstances. And even if a fluid pulse is released during every stronger seismic sequence its volume might not be sufficient to reach the Earth's surface with a detectable amplitude. This is also directly related to the pressure buildup in the fluid reservoir beneath the sealed fault, which is a long-lasting process and thus earthquakes that occur soon after releasing the accumulated fluid pressure are likely to not be accompanied by a significant fluid release.

In this context it is also of interest to consider the *hypocenter cluster geometry* in 3D and its relation to the presence of permeable channels in a shallow crust allowing crustal fluids to reach the surface. In Fig. 9 hypocenters of individual earthquake sequences are indicated in a vertically oriented cross section and show a hat-like structure in depths from 6.0 to 10.5 km extending about 10 km north-south. The Hartoušov mofette field is located about 10 km south from the center of the main cluster, which corresponds to 6 km distance from its southern tip. A pronounced segmentation of the fault plane is apparent with the 2008 and 2014 segments in the southern branch of the cluster and the 2011, 2017 and 2018 segments clusters in its northern branch. It is worth noting that the 2014 mainshocks showed unfavorable oriented focal mechanisms and occurred on a fault jog activated by stress concentration resulting from previous swarm activity (Hainzl et al., 2016, Jakoubková et al. 2018). This structural and possibly impermeable boundary within the fault zone was broken by the M_L 3.5 mainshock of the 2014 sequence - the first earthquake of this sequence which was followed by the massive CO_2 flow rise in Hartoušov.

Recently, since the summer of 2019, the CO_2 flow rate in Hartoušov F1 has decreased below 10 L/min, which could be a sign of the approaching occurrence of a new seismic swarm, according to the Sibson's fault valve model. However, one should also take into account that the flow rate decrease in 2019 could have been caused by the drought period in the summer. The reduced groundwater pressure in the whole area would lead to the rise of the diffuse component of gas flow reducing the gas discharge in the borehole. Comparing the records of groundwater level in nearby mofettes with the gas flow rate in the F1 borehole however gives unequivocal results. While some correlation between gas flow and water level was found for 2018 and 2019, the gas flow rate in 2017 was found independent of the water level in mofettes.

The clear coseismic CO_2 flow rate increase during the 2008 and 2014 seismic sequences indicates the presence of a *permeable channel between the southern cluster and the Hartoušov mofette field* (Fig. 9). The absence of CO_2 flow anomalies coinciding with the seismic activity in northern clusters could be interpreted to show that the hydraulic connection between these fault patches and the Hartoušov mofette is missing, which could be related to the afore-mentioned fault jog. Besides, it is also of interest that epicenter distribution and CO_2 degassing occurrence is typically separated in the area (Weinlich et al., 2006; Babuška and Plomerová, 2008); most earthquakes occur in the northern, CO_2-free part of the Cheb Basin.

Other monitored sites such as Bublák and Soos show, similar to Hartoušov, almost constant CO_2 discharge since early 2017. As these stations were not in operation during the 2008 and 2014 seismic sequences showing coseismic CO_2 increase in Hartoušov, no inferences about their correlation to the seismic activity can be drawn. Bubble fractions derived from resistivity measurements of the water-bubble system are found quite stable. For the measurement period of four years no maintenance of the probe was required and, compared to the pressure difference method, the system

Deleted: ¶

is less sensitive to the depth of the probe below the water table. However, no seismogenic anomaly of as flow rate has occurred yet that could be used to calibrate the system. Continuous monitoring of CO_2 degassing is required to determine whether future seismic activity in the southern cluster will generate an increase in degassing in either of the monitored sites and enable the verification of the hypothesis that only earthquakes in the southern cluster are capable of generating a CO_2 pulse which reaches the surface.

5. Conclusions

The present study is focused on the long-term monitoring of CO_2 degassing in the form of mofettes and gaseous mineral springs targeted on the West Bohemia/Vogtland region in Central Europe, which is typified by the occurrence of earthquake swarms and discharge of carbon dioxide of magmatic origin. The gas flow measurement is applied to two types of sources: natural wet mofettes with gas outflow through surface water pools and boreholes tapping shallow CO_2-saturated aquifers. The different local conditions of the five monitored sites call for different methods of gas capture and flow rate measurement. Besides the direct flow measurement using a drum chamber gas flowmeter, electronic MEMS flowmeters and Venturi-based probes we introduce a novel, indirect method based on quantifying the gas bubble contents in a water column, which is capable of functioning in severe environmental conditions. The method is based on measuring the pressure difference along a fixed depth interval in a water column, which is proportional to the mean bubble fraction within the measured section. We analyze the dependence of the bubble fraction on depth and project it to the atmospheric pressure to make it directly comparable to the gas flow rate. Laboratory tests indicate the nonlinear dependence of the bubble fraction on the flow rate, which is confirmed by empirical models found in the chemical and nuclear engineering literature. Flow rates and bubble fractions observed in a pilot borehole F1 in the Hartoušov mofette show a high mutual correlation, however some discrepancy is found between the measured flow rate and that predicted by the empirical models. This discrepancy calls for further analysis.

We also analyzed the long-term monitoring of gas flow and bubble fraction in the pilot borehole for the period 2008 – 2019. We found a quite strong barometric influence on the hydraulic head of the confined aquifer corresponding to a barometric efficiency of 0.76, which can be attributed to the compressibility of the pore fluids including the gaseous phase of carbon dioxide.

The record of gas flow rate and bubble fraction in Hartoušov F1 shows two high-amplitude coseismic rises coinciding with the occurrence of earthquake swarms in 2008 and 2014. The flow rate increased to a multitude of the preseismic level for several months and was followed by a long-term decay. However, another three seismic swarms occurring in the same fault zone were not associated with any significant CO_2 flow anomaly. We surmise that this may be related to the slightly farther location of hypocenters of these swarms in comparison with the two which caused the coseismic CO_2 flow rise. Further long-term CO2-flow monitoring is required to verify the mutual influence of CO_2 degassing and seismic activity in the area.

Deleted: emanations

Code/Data availability

Most of the data analyzed in the manuscript including email address for requesting additional data are available online at web.natur.cuni.cz/uhigug/carbonnet/en_index.html .

Author's contribution

VB and TF designed and carried out the measurements and ML formulated the theoretical part with support of TF. TF prepared the manuscript with contributions from all co-authors.

Competing interests

The authors declare that they have no conflict of interest.

Acknowledgments

CO2 flow monitoring and the work of the authors was supported by the project CzechGeo/EPOS-Sci (CZ.02.1.01/0.0/0.0/16_013/0001800). The authors thank also to Jan Vilhelm for valuable ideas.

694 **References**

695

696 Acworth R.I. and Brain T., Calculation of barometric efficiency in shallow piezometers using water levels,
697 atmospheric and earth tide data. Hydrogeology Journal 16, 1469–1481, 2008.

698 Babuška V., Plomerová J., Control of paths of quaternary volcanic products in Western Bohemian Massif by
699 rejuvenated variscan triple junction of ancient microplates. Stud. Geophys. Geod., 52, 607-629, 2008.

700 Babuška, V., et al., Origin of earthquake swarms in the western Bohemian Massif: Is the mantle CO_2 degassing,
701 followed by the Cheb Basin subsidence, an essential driving force?, Tectonophysics 668-669, 42-51,
702 http://dx.doi.org/10.1016/j.tecto.2015.12.008, 2016.

703 Bachura, M. and Fischer T., Detailed velocity ratio mapping during the aftershock sequence as a tool to monitor the
704 fluid activity within the fault plane. Earth and Planetary Science Letters 453, 215–222.
705 https://doi.org/10.1016/j.epsl.2016.08.017, 2016.

706 Bankwitz, P., Schneider, G., Kämpf, H., Bankwitz, E., Structural characteristics of epicentral areas in Central Europe:
707 study case Cheb Basin (Czech Republic). J. Geodyn. 35, 5–32, 2003.

708 Baubron, J. C., Allard P., Toutain J. P., Diffuse volcanic emissions of carbon dioxide from Vulcano island, Italy,
709 Nature, 344, 51–53, 1990.

710 Bräuer, K., Kämpf, H., Strauch, G., Weise, S.M., Isotopic evidence ($^3He/^4He$, ^{13}C CO_2) of fluid-triggered intraplate
711 seismicity. J. Geophys. Res. 108 (B2), 2070. http://dx.doi.org/10.1029/2002JB002077, 2003.

712 Bräuer, K., Kämpf, H., Niedermann, S., Strauch, G., Tesař, J., Natural laboratory NW Bohemia: comprehensive fluid
713 studies between 1992 and 2005 used to trace geodynamic processes. Geochem. Geophys. Geosyst. 9.
714 http://dx.doi.org/10.1029/ 2007GC001921 (Q04018), 2008.

715 Bussert R., Kämpf H., Flechsig C., Hesse K., Nickschick T., Liu Q., Umlauft J., Vylita T., Wagner D., Wonik T.,
716 Flores H.E., and Alawi M., Drilling into an active mofette: pilot-hole study of the impact of CO_2-rich mantle-derived
717 fluids on the geo–bio interaction in the western Eger Rift (Czech Republic). Sci. Dril., 23, 13–27,
718 https://doi.org/10.5194/sd-23-13-2017, 2017.

719 Camarda, M., S. Gurrieri, and M. Valenza., CO_2 flux measurements in volcanic areas using the dynamic concentration
720 method: Influence of soil permeability, J. Geophys. Res., 111, B05202, doi:10.1029/2005JB003898, 2006.

721 Dahm, T., Fischer, T., Velocity ratio variations in the source region of earthquake swarms obtained from arrival time
722 double-differences. Geophys. J. Int. 196, pp. 957-970. URL: http://dx.doi.org/10.1093/gji/ggt410, 2014.

723 Dmytriw, A. M., Kilian, W. T., Speldrich, J. W., Beck, S. E., Morales, G., and Gehman, R. W., U.S. Patent No.
724 7,278,309. Washington, DC: U.S. Patent and Trademark Office, 2007.

Formatted: Subscript

Formatted: Subscript

Formatted: Subscript

Faber, E., Horálek, J., Boušková, A., Teschner, M., Koch, U., and Poggenburg, J., Continuous gas monitoring in the West Bohemian earthquake area, Czech Republic: First results. Studia Geophysica et Geodaetica, 53(3), 315-328, 2009.

Fischer, T., Horálek, J., Slip-generated patterns of swarm microearthquakes from West Bohemia/Vogtland (central Europe): evidence of their triggering mechanism. J. Geophys. Res. 110, B05S21. http://dx.doi.org/10.1029/2004JB003363, 2005.

Fischer, T., Horálek, J., Hrubcová, P., Vavryčuk, V., Bräuer, K., Kämpf, H., Intra-continental earthquake swarms in West-Bohemia and Vogtland: a review, Tectonophysics 611, 1-27, doi: 10.1016/j.tecto.2013.11.001, 2014.

Fischer, T., Matyska, C., and Heinicke., Earthquake-enhanced permeability–evidence from carbon dioxide release following the ML 3.5 earthquake in West Bohemia. Earth and Planetary Science Letters, 460, 60-67, 2017.

Franke, W., The mid-European segment of the Variscides: tectonostratigraphic units, terrane boundaries and plate tectonic evolution. In: Franke, W., Haak, V., Oncken, O., Tanner, D. (Eds.), Orogenic Processes: Quantification and Modelling in the Variscan Belt, vol. 179. Geol. Soc., Spec. Publ., London, pp. 35–61, 2000.

Geissler, W.H., Kämpf, H., Kind, R., Klinge, K., Plenefisch, T., Horálek, J., Zedník, J., Nehybka, V., Seismic structure and location of a CO_2 source in the upper mantle of the western Eger rift, Central Europe. Tectonics 24 (TC5001. http://dx.doi.org/10. 10292004TC001672), 2005.

Ghiaasiaan, M.S., Two-phase flow, boiling and condensation in conventional and miniature systems. Cambridge University Press. 636p, 2008.

Gurrieri, S., Valenza M., Gas transport in natural porous medium: a method for measuring soil CO_2 flows from the ground in volcanic and geothermal areas, Rend. Soc. Ital. Mineral. Petrol., 43, 1151–1158, 1988.

Hainzl, S., Fischer, T., Indications for a successively triggered rupture growth under – lying the 2000 earthquake swarm in Vogtland/NW-Bohemia. J. Geophys. Res. 107 (B12), 2338. http://dx.doi.org/10.1029/2002JB001865, 2002.

Hainzl, S., Fischer, T., Čermáková, H., Bachura, M., Vlček, J., Aftershocks triggered by fluid-intrusion: evidence for the aftershock sequence occurred 2014 in West Bohemia/Vogtland. J. Geophys. Res., Solid Earth 121. http://dx.doi.org/ 10.1002/2015JB012582, 2016

Heinicke, J., Koch, U., Slug flow — a possible explanation for hydrogeochemical earthquake precursors at Bad Brambach, Germany. Pure Appl. Geophys. 157 (10), 1621–1641, 2000.

Horálek, J., Šílený, J., Fischer, T., Moment tensors of the January 1997 earthquake swarm in NW Bohemia (Czech Republic): double-couple vs. non-double-couple events. Tectonophysics 356, 65–85, 2002.

Hron J., and Škuthan B., Continuing research into the pressure field of carbon-dioxide in the West-Bohemian spa region (in Czech). Czech Ministry of Environment, Prague, 112 p, 2006.

Deleted: Ellingsen, K., and Risso, F., On the rise of an ellipsoidal bubble in water: oscillatory paths and liquid-induced velocity. Journal of Fluid Mechanics, 440, 235-268, 2001.

Deleted: ¶

Formatted: Subscript

Formatted: Subscript

Hrubcová, P., Geissler, W.H., Bräuer, K., Vavryčuk, V., Tomek, Č., Kämpf, H., Active magmatic underplating in western Eger Rift, Central Europe. Tectonics 36. https://doi.org/10.1002/2017TC004710, 2017.

Jacob C.E., Fluctuations in artesian pressure produced by passing railroad-trains as shown in a well on Long Island, New York. Eos Trans. AGU, 20(4), 666– 674, doi:10.1029/TR020i004p00666, 1939.

Jakoubková, H., Horálek, J., and Fischer, T., 2014 mainshock-aftershock activity versus earthquake swarms in West Bohemia, Czech Republic. Pure and Applied Geophysics, 175(1), 109–131. https://doi.org/10.1007/s00024-017-1679-7, 2018.

Kämpf, H., Geissler, W.H., Bräuer, K., Combined gas-geochemical and receiver func- tion studies, of the Vogtland/NW-Bohemia intraplate mantle degassing field Central Europe. In: Ritter, J.R.R., Christiansen, U.R. (Eds.), Mantle Plumes — A Multidisciplinary Approach. Springer-Verlag, Berlin-Heidelberg-New York, pp. 127–158., 2007.

Koch, U., Heinicke, J., and Voßberg, M., Hydrogeological effects of the latest Vogtland-NW Bohemian swarmquake period (August to December 2000). Journal of Geodynamics, 35(1), 107-123, 2003.

Montoya, G.; Lucas, D.; Baglietto, E.; Liao, Y., A review on mechanisms and models for the churn-turbulent flow regime. Chem. Eng. Sci. 141, 86-103. DOI 10.1016/j.ces.2015.09.011, 2016.

Nickschick T., Kämpf H., Flechsig C., Mrlina J., Heinicke J., CO_2 degassing in the Hartoušov mofette area, western Eger Rift, imaged by CO_2 mapping and geoelectrical and gravity surveys. Int J Earth Sci., 2015.

Roeloffs, E., Poroelastic techniques in the study of earthquake=related hydrologic phenomena, Advances in Geophysics, 37, 135-195, 1996.

Rojstaczer, S. and Riley F. S., Response of the water level in a well to Earth tides and atmospheric loading under unconfined conditions. Water Resources Research, 26 (8), 1803-1817, 1990.

Sander, R., Compilation of Henry's law constants (version 4.0) for water as solvent. Atmos. Chem. Phys., 15, 4399-4981, DOI 10.5194/acp-15-4399-2015, 2015.

Sibson, R.H., Implications of fault-valve behavior for rupture nucleation and recurrence. Tectonophysics 211, 283–293, 1992.

Škuthan B., Hron J., Pěček J. and Keprta M., Carbon dioxide field in the West Bohemian Spring Region: Introductory results. Bull. Czech Geol. Surv., 76/4, 203−208, 2001.

Špičák, A., Horálek, J., Migration of events during the January 1997 earthquake swarm (The West Bohemia–Vogtland region). Stud. Geophys. Geod. 44, 227–232, 2000.

Špičáková, L., Uličný, D., Koudelková, G., Tectonosedimentary evolution of the Cheb Basin (NW Bohemia, Czech Republic) between Late Oligocene and Pliocene: a preliminary note. Studia Geophys. Geod. 44, 556–580, 2000.

Todd D.K., 1980. Groundwater Hydrology. 2d ed. New York: John Wiley & Sons.

Formatted: Subscript

Formatted: Subscript

792 Vavryčuk, V., Non-double-couple earthquakes of January 1997 in West Bohemia, Czech Republic: evidence of tensile
793 faulting. Geophys. J. Int. 149, 364–373. http://dx.doi.org/10.1046/j.1365-246X.2002.01654.x, 2002.

794 Vavryčuk, V., Principal earthquakes: theory and observations from the 2008 West Bohemia swarm. Earth Planet. Sci.
795 Lett. 305, 290–296. http://dx.doi.org/10.1016/ j.epsl.2011.03.002, 2011.

796 Vavryčuk, V., and P. Hrubcová, Seismological evidence of fault weakening due to erosion by fluids from observations
797 of intraplate earthquake swarms, J. Geophys. Res. Solid Earth, 122, doi:10.1002/2017JB013958, 2017.

798 Weinlich, F.H., Bräuer, K., Kämpf, H., Strauch, G., Tesar, J., Weise, S.M., An active sub – continental mantle volatile
799 system in the western Eger rift, Central Europe: gas flux, isotopic (He, C, and N) and compositional fingerprints.
800 Geochim. Cosmochim. Acta 63, 3653–3671. http://dx.doi.org/10.1016/S0016-7037(99)00187-8, 1999.

801 Weinlich, F. H., Faber, E., Boušková, A., Horálek, J., Teschner, M., and Poggenburg, J., Seismically induced
802 variations in Mariánské Lázně fault gas composition in the NW Bohemian swarm quake region, Czech Republic—A
803 continuous gas monitoring. Tectonophysics, 421(1), 89-110, 2006.

804 Ziegler, P.A., European Cenozoic rift system. Tectonophysics 208, 91–111, 1992.

805 Zuber, N., and Findlay, J., Average volumetric concentration in two-phase flow systems. Journal of heat transfer,
806 87(4), 453-468, 1965
807

808

809

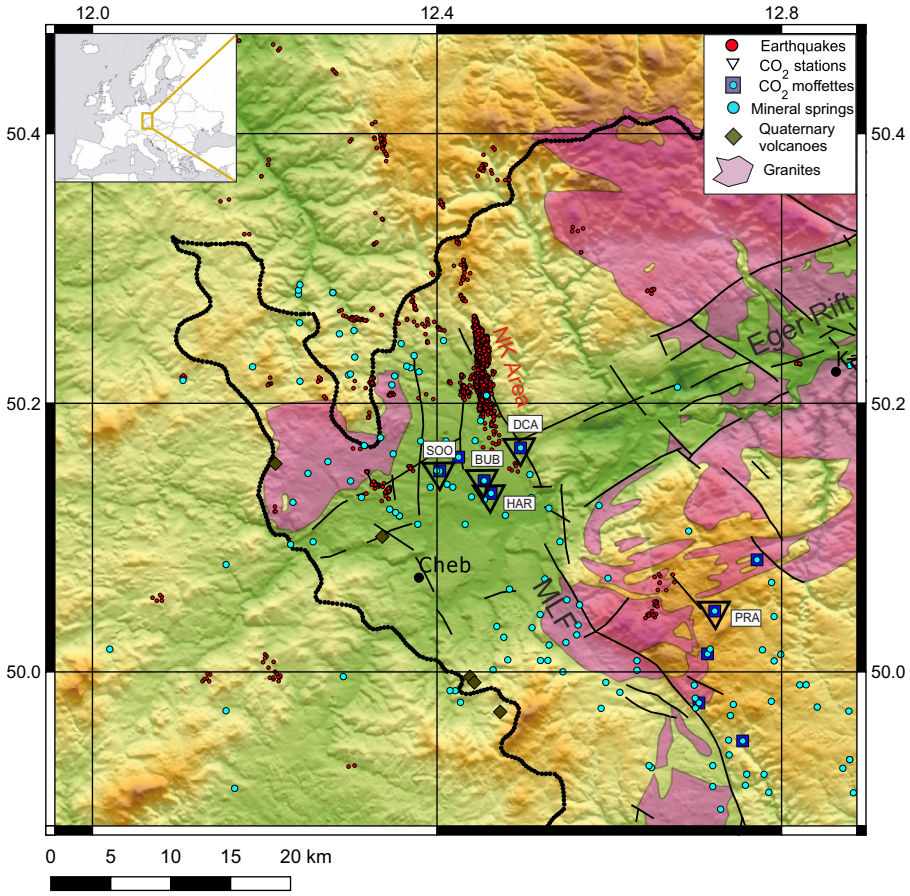

Figure 1. Relief map of the West Bohemia/Vogtland region with the fault network, granite units, and major fault zones as Mariánské Lázně Fault (MLF) and Eger Rift. Seismic events, major focal zone of Nový Kostel (NK Area), CO_2 monitoring stations, CO_2 mofettes and mineral springs and Quaternary volcanoes are also indicated (see the legend).

Figure 2. Photos of selected CO_2 monitoring fields – Hartoušov, SOOS, Bublák and Prameny

Formatted: Subscript

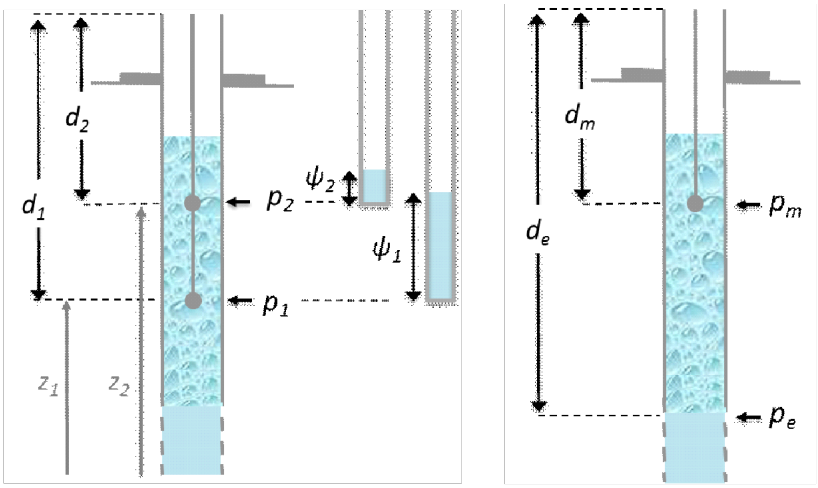

a) b)

Figure 3. Measurement of pressure in the borehole with ascending bubbles: the measured pressure p and the related pressure head ψ at two different depths d_1 and d_2 within the bubble column using the *differential method* (a); pressure within the bubble column p_m and beneath p_e used to determine the mean bubble fraction using the *integral method* (b). Note that the difference of altitudes $z_2 - z_1 = d_e - d_m$.

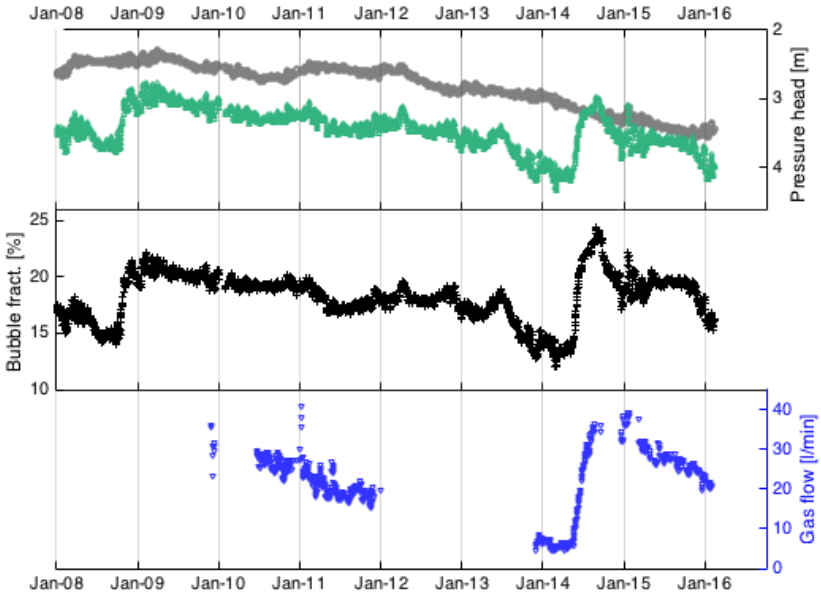

Figure 4. Daily averages of the reference pressure head h_e (grey) unaffected by gas flow and in the monitored Hartoušov F1 well, h_m (green); the volumetric fraction of bubbles (black) determined by Eq. 4 and CO_2 flow (blue) in the Hartoušov F1 well for the period 2008-2016. Because no reference pressure measurement below the bubble entry point was available for the studied period, a pressure head in nearby Hrzín borehole, which was free of gas flow, was used as h_e.

Deleted: in the reference well

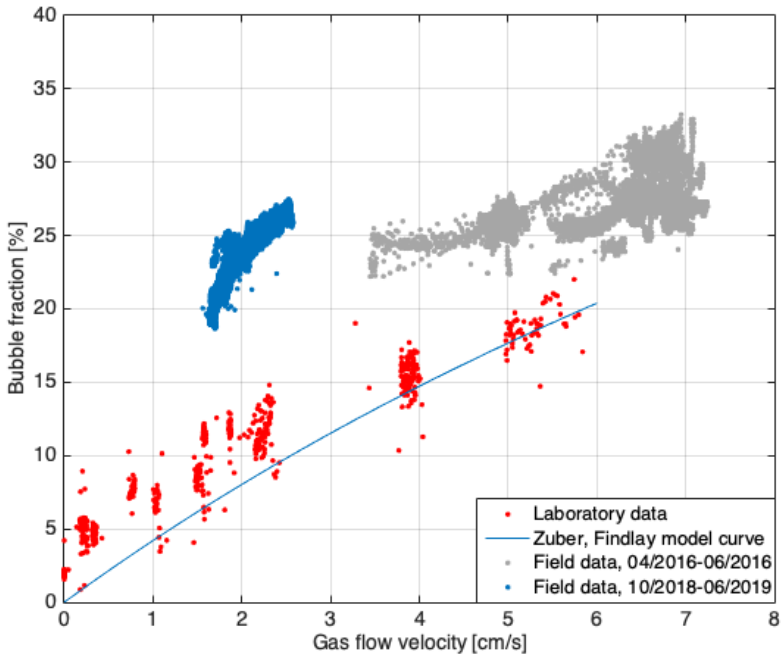

844

845 Figure 5. Comparison of gas flow velocity and volumetric fraction of bubbles for the field (Hartoušov mofette) and laboratory
846 measurement. Laboratory measurements are smoothed by RC circuit of 30 s time constant (red points) and additionally by running
847 average of 1 min length; the field measurements from 2016 (grey points) are based on the differential method with sensor distance
848 of 1.0 m; the field measurements from 2018-2019 (blue points) are based on the integral method. Blue line is the best fit based on
849 eq. (5).

850

851

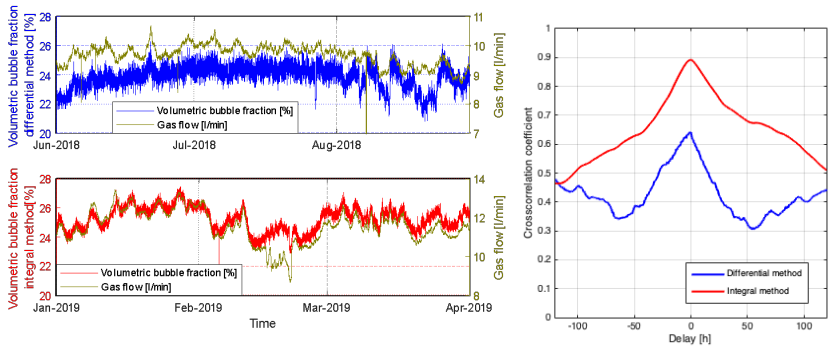

852

853 Figure 6. Comparison of volumetric bubble fraction derived using differential (top left) and integral (bottom left) methods with the
854 gas flow at the Hartoušov F1 borehole. Depth of pressure probes for the differential method are 4.45 and 5.45 m below the surface.
855 For the integral method it is 5.45 m and 27.2 m. On the right the cross-correlation functions between the bubble fraction and gas
856 flow rate are shown.

857

Deleted: integral and

Deleted: site

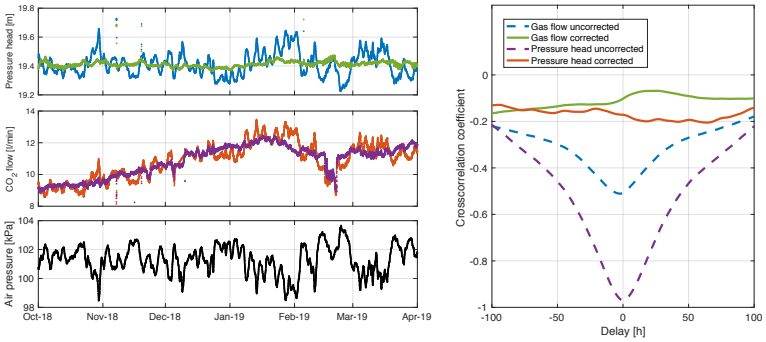

a) b)

Figure 7. The barometric effect to the pressure head and CO_2 flow in the Hartoušov F1 borehole for the period from October 2018 to April 2019. a) Original measurements are indicated in blue and those corrected for barometric pressure are in red. The upper panel shows pressure head at the depth below the bubble formation and the lower panel shows gas flow measured by flowmeter. The success of barometric correction is illustrated in b) showing the decrease of barometric anticorrelation after correcting.

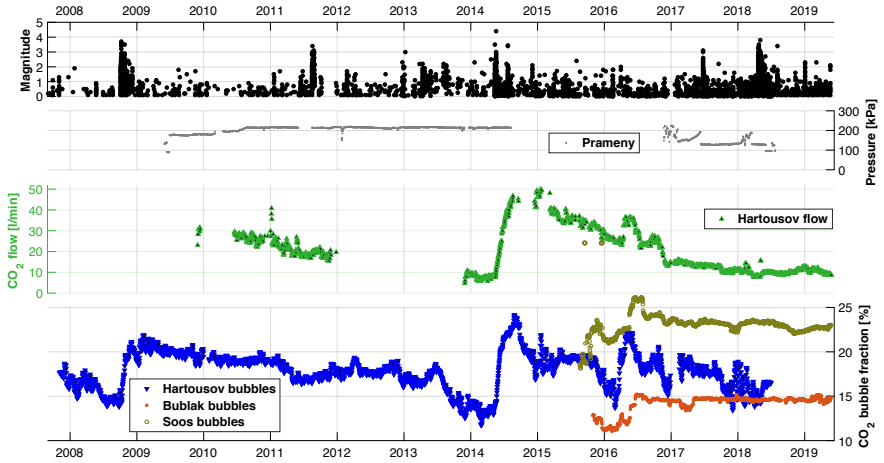

a)

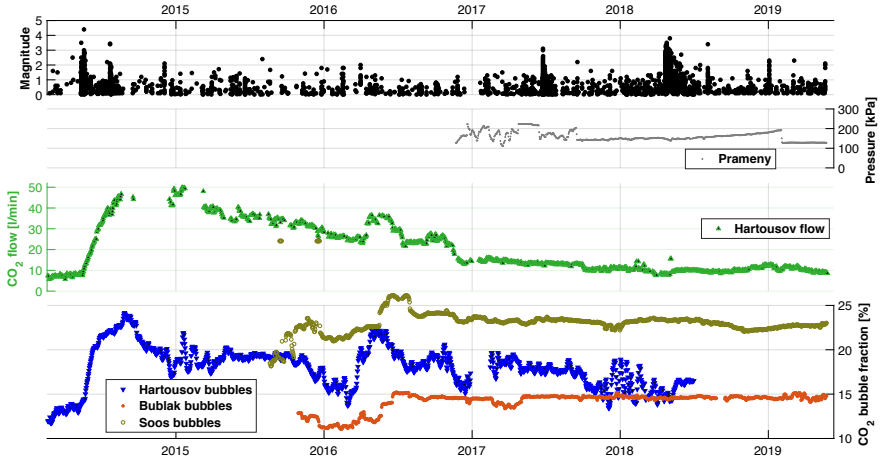

b)

Figure 8. Comparison of seismic activity and CO_2 production at individual monitoring sites in West Bohemia. For Hartoušov F1 the CO_2 flow and gas bubble fraction are shown; for Bublák and Soos the CO_2 bubble fraction is shown and for Prameny the gas pressure in a closed borehole is plotted; (a) period 2007-2019; (b) detail for the period 2014-2019. Gas bubble fraction was determined using the pressure difference method in the integral version for Hartoušov (blue), in differential version for Bublák (red) and by the resistivity method for Soos (light brown).

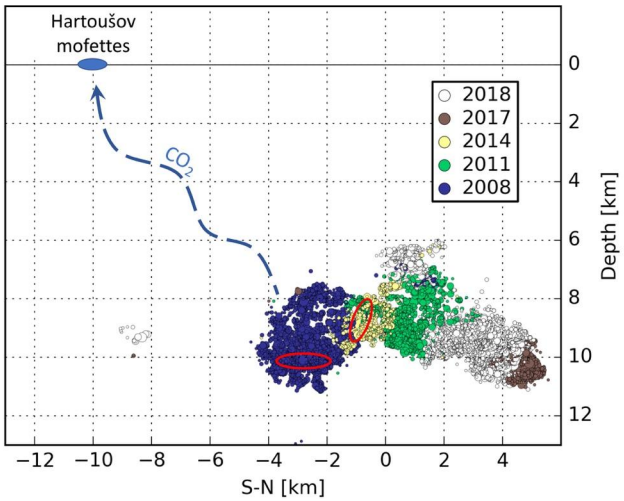

Figure 9. Vertical, north-south oriented section through the Nový Kostel fault zone with hypocenters of the earthquake swarms occurred between 2008 and 2018. The position of the Hartoušov mofette showing coseismic CO_2 flow rate increase is indicated on the surface. Red ovals show the position of first events of the 2008 and 2014 seismic sequences.

Page 13: [1] Deleted **Tomáš Fischer** **07/04/2020 13:11:00**